ULTRASTRUCTURAL LOCALIZATION OF HISTIDINE-RICH GLYCOPROTEIN IN SKELETAL MUSCLE FIBERS: CO-LOCALIZATION WITH AMP DEAMINASE

L. Mattii, F. Bianchi, A. Falleni, S. Frascarelli, M. Masini, G. Alì, G. Chiellini, and A.R.M. Sabbatini

Dipartimento di Medicina Clinica e Sperimentale, Università di Pisa, Pisa, Italy (LM, FB, AF)

Dipartimento di Patologia Chirurgica, Medica, Molecolare e dell'Area Critica, Università di Pisa, Pisa, Italy (SF, GC, ARMS)

Dipartimento di Ricerca Traslazionale e delle Nuove Tecnologie in Medicina e Chirurgia, Università di Pisa, Pisa, Italy (MM)

U.O. Anatomia Patologica III, Azienda Ospedaliero-Universitaria Pisana (AOUP), Pisa, Italy (GA)

Nutrafood, Centro Interdipartimentale di Ricerca Nutraceutica e Alimentazione per la salute (LM)

Corresponding author: Antonietta R.M. Sabbatini, M.D., Dipartimento di Patologia Chirurgica, Medica, Molecolare e dell'Area Critica, Università di Pisa, via Roma 55, 56126 Pisa, Italy.

Phone: +39.050.2218-674, Fax: +39.050.2218-660, E-mail: antonietta.sabbatini@med.unipi.it

Running headline: HRG immunolocalization in skeletal muscle by TEM

ABSTRACT

Histidine-rich glycoprotein (HRG) is a plasma protein synthesized by liver. We have given the first evidence of a tissue localization of HRG demonstrating its presence in skeletal muscle, associated to the zinc enzyme AMP deaminase (AMPD1). Moreover, we have shown that muscle cells do not synthesize HRG but they can internalize it from plasma. We have recently demonstrated by confocal laser scanning microscopy that, in human skeletal muscle, HRG is mainly localized in the myofibrils, preferentially at the I-band of the sarcomere, in sarcoplasm and in the nuclei. Using transmission electron microscopy (TEM) and immunogold analysis, we carried out the present study on human and rat normal skeletal muscle with the purpose to deepen the ultrastructural localization of HRG in skeletal muscle fibers.

The immunogold analysis evidenced the presence of HRG in the sarcomeres, mainly in the I-band and in a minor extent in the A band, in the heterochromatin of nuclei and in the sarcoplasmic reticulum. The co-localization of HRG and skeletal muscle AMP deaminase (AMPD1) was also analysed. A co-labeling of HRG and AMPD1 was evident at sarcomeric, sarcoplasmic reticulum and nuclear level. The significance of these interesting and new results is discussed in the present paper.

Keywords: muscle biopsies, immunohistochemistry, sarcomere, nucleus, metallochaperone, AMP deaminase

INTRODUCTION

Histidine-rich glycoprotein (HRG) is a single chain, 75 kDa plasma protein synthesized by parenchymal liver cells (1). Plasma is the major pool of HRG (100-150 μg/ml) although it was also found in colostrum, milk and infant urine as well as in megakaryocytes, platelet α-granules and immune cells (2, 3, 4). HRG has a multidomain structure consisting of three distinct parts: the N-terminal, that contains two cystatin–like N-terminal domains (N1 and N2), the central part containing a unique histidine/proline rich domain and the C-terminal domain (5). The most salient feature of the protein is its unusually high content of both histidine and proline residues. Moreover, it contains approximately 14% carbohydrate attached to six N-linked glycosylation sites (1). The multidomain structure of HRG and its ability to bind a wide range of ligands (e.g. divalent metal cations, heparin, heparan sulfate, plasminogen, fibrinogen, IgG, complement) (6, 7, 8, 9, 10) as well as different cell surface receptors such as FcγR, heparan sulfate, tropomyosin (11, 12), suggest a multivalent function of the protein. Indeed, the data of literature clearly demonstrate the involvement of HRG in the modulation of a number of important biological processes such as blood coagulation, complement activation, immunocomplex clearance, angiogenesis, cell adhesion and migration, phagocytosis of apoptotic cells (13).

We have discovered a HRG protein in rabbit skeletal muscle (14) while we were carrying out studies on AMP deaminase (AMPD1), a zinc enzyme that catalyzes the hydrolytic deamination of AMP to IMP and ammonia (15). Moreover, we found that muscle HRG was associated to AMPD1 and it was critical in assuring both the molecular integrity and the activity of the enzyme. Like the plasma protein, muscle HRG could bind zinc (16). The existence in muscle HRG of a specific zinc binding site has been later confirmed by X-ray absorption spectroscopy analysis (17) permitting to envisage the addition of this protein into the family of metallochaperones, soluble proteins that function as intracellular shuttles for metal ions: they acquire the metal ion and deliver it to specific partner proteins (18). In this view, HRG could enhance the in vivo stability of metalloenzymes such as AMPD1 (17).

We have also detected HRG in human skeletal muscle where it was mainly localized in type IIB fibers, that contain the higher level of AMPD1 when compared to type I and IIA fibers (19). Moreover, a positive correlation between the muscle content of HRG and the level of AMPD1 activity has been shown by an immunohistochemical study on skeletal muscle of patients affected by AMPD1 deficiency (20). Interestingly, we have demonstrated by an in vitro study on rhabdomyosarcoma cell line that muscle HRG is not synthesized by muscle cells but they can internalize it (21). Therefore, we have given evidence, for the first time, that plasma HRG can be carried to skeletal muscle, and probably also to other tissues, via circulation. Our finding has been later confirmed by Tugues et al (22) through in vivo experiments performed with radiolabeled HRG. They showed that, after intravenous injection, HRG was internalized quickly in healthy tissues, including muscle, and in tumors. The HRG cellular localization has been recently investigated by our group in normal human skeletal muscle by the use of optical and confocal microscopy (23). We observed a diffuse, uniform immunoreactivity for HRG in the connective tissue among the muscle fibers and, in muscle fibers, a preferential distribution of the protein in the sarcomere, mainly in the I-band. A HRG positivity was also evidenced in the nuclei.

The aim of the present study was to deepen the-subcellular localization of HRG in skeletal muscle fiber. For this purpose, the ultrastructural distribution of HRG was studied by TEM immunogold analysis using human and rat skeletal muscles. TEM analysis allowed us to better understand the relationship between HRG and the cellular compartments such as nuclear chromatin, organelles, sarcoplasmic reticulum and sarcoplasm. In addition, the HRG distribution was also compared with that of AMPD1.

MATERIALS AND METHODS

Antibodies and reagents

Rabbit anti-human HRG polyclonal antibody (HRG-462) raised against the C-terminal region (residues 462-471) of plasma HRG and rabbit anti-human AMPD1 polyclonal antibody were produced

in-house as previously described (19,20). Rabbit anti-rat HRG polyclonal antibody was purchased from Cloude–Clone Corp (Katy, Texas, USA). Goat anti-rabbit 10 nm and 20 nm gold-conjugated antibodies were purchased from Ted Pella Inc (Redding, California, USA) and from British Biocell International (Cardiff, UK), respectively. All other reagents were of analytical grade and were purchased from Sigma-Aldrich and Fluka (Buchs, Switzerland).

Human Sample collection

Three human muscle biopsies, one from gastrocnemius (male, patient age = 28), and two from quadriceps femoris (females, patient age = 69 and 78), were selected from the archives of Division of Pathology, Department of Surgical, Medical, Molecular Pathology and Critical Care, University of Pisa because they were healthy controls coming from surgery for fracture resolution. Each one was preserved both frozen and Epon/Durcupan embedded. Serial sections of 8 μm were cut from frozen biopsies and processed for routine histological and histochemical stains, i.e. hematoxylin-eosin, succinate dehydrogenase activity (SDH), NADH tetrazolium reductase (NADH-TR), routine ATPase (pH 9.4), ATPase pre-incubated at pH 4.3 and 4.6 (24). Semi- and ultra-thin sections were cut from Epon/Durcupan embedded biopsies for TEM analysis.

Rat sample collection

Muscle biopsies from biceps femoris were taken from two male Wistar rats and embedded both in paraffin for routine hematoxylin-eosin staining and in Poly/Bed 812 for TEM analysis. In particular, after removal, rat samples were immediately trimmed into small blocks (1 mm^3), fixed in 1% (w/v) glutaraldehyde-4% (w/v) formaldehyde (freshly obtained from paraformaldehyde) in phosphate buffer solution (0.1 M pH 7.2) (PBS) for 4 h at 4C and, after washing in the same buffer, the specimens were post-fixed in 1% (w/v) OsO_4/PBS for 2 h. Samples were also fixed in 4% paraformaldeide/PBS for 4 h at 4C omitting the post-fixation step in 1% (w/v) OsO_4/PBS. All samples were then washed in distilled water and dehydrated with a graded series of ethanol before transferring the specimens to propylene oxide for 6 min. Finally, Poly/Bed 812 embedding in flat mold at 60C for 48 h was carried out and semi- and ultra-thin sections were cut for TEM analysis.

A rat liver sample was submitted to the procedure above described and used as tissue positive control.

TEM and Immunogold analysis

In order to assess the specimen quality and orientation, a number of semi-thin sections were stained with toluidine blue and observed by light microscopy. Ultrathin sections (60–80 nm-thick) were obtained with a diamond knife, placed on 200- mesh formvar/carbon coated nickel grids and allowed to dry. Some sections were counterstained with uranyl acetate and lead citrate and observed with a Jeol JEM-100SX transmission electron microscope (Jeol, Tokyo, Japan) at 80 kV, in order to assess their quality.

For the immunogold analysis, all the steps were performed at room temperature using the Basic Buffer Solution (BBS) containing 0.4M NaCl in PBS (pH 7.2) to avoid non-specific antibody binding. The grids with the sections face-down were placed on a droplet of saturated aqueous $NaIO_4$ solution. After five washes in BBS, the sections were treated with 0.5 M NH_4Cl, transferred onto a droplet of 10% BSA–BBS and then incubated overnight at 4C in a moistened chamber with anti-human (HRG-462 1:3000) or anti-rat HRG (1:50) polyclonal antibodies in 1% BSA–BBS. The sections were then washed with 1% BSA–BBS and incubated with the gold conjugated secondary antibody (10 nm or 20 nm gold particles for rat and human HRG detection, respectively) diluted 1:30 in 5% FBS, 0.1% BSA, 0.05% Tween 20 in BBS. Grids were jet-washed with BBS and fixed in 1% glutaraldehyde for 3 min. Sections were finally jet-washed in distilled water and counterstained with uranyl acetate and lead citrate (25, 26).

For the double immunogold staining performed in human samples, before fixing the samples in 1% glutaraldehyde, an additional incubation with anti AMPD1 primary antibody (overnight at 4C), followed by the incubation with 10 nm gold conjugated secondary antibody diluted 1:30, was performed. Negative controls for secondary antibodies were performed omitting primary antibodies and incubating the specimens with nonimmune serum.

To better understand the HRG distribution at sarcomeric level, a semi-quantitative analysis was performed in human samples. Specifically, counting of immunogold particles (20 nm) placed inside the sarcomeres was carried out by transmission electron microscopy at 15000X magnification. This magnification corresponds to the minimal magnification at which gold particles and sarcomeres can be

detected concomitantly. Grid squares containing labeled sarcomeres were chosen randomly for the count as random selection makes the quality of the scanning independent from intensity of gold labeling. In these squares, only longitudinal sections of sarcomeres were used to display their real sizes. In particular, starting at a grid square corner, the entire sarcomere within that grid square was scanned. In each sarcomere, the number of gold particles was counted, and we expressed the mean value of immunogold particles for I-band (MV_I) or A-band (MV_A) out of 20 sarcomeres counted. The related density values (δMV_I and δMV_A), corresponding to the mean number of gold particles/μm^2, were worked out.

Statistics

The density values were obtained in 20 sarcomeres/grid; total number of grids was 30 (10 grids per each human biopsy), which were collected from three separate experiments. Data are reported as the $\delta MV \pm SD$. Inferential statistics to compare groups were carried out by using Student's t test (null hypothesis was rejected for $P \leq 0.05$).

RESULTS

The human skeletal muscle biopsies used for the experiments showed no histological or histochemical abnormalities. Indeed, on the examination by optical microscopy the histochemical stains, commonly used for the assessment of pathological samples, evidenced profiles of normal muscle in all the three biopsies. Moreover, the muscle fibers appeared highly contracted in all samples.

The rat specimens also showed no histological abnormalities on examination by optical microscopy. While the anti human HRG antibody specificity was already demonstrated (19), the specificity of the anti rat HRG antibody was ascertained in the present work by immunofluorescence microscopy. In particular the immunoreactivity of rat skeletal muscle fibers was comparable to the pattern obtained on human skeletal muscle by the anti human HRG antibody (data not shown).

For TEM immunogold analysis, positive and negative controls were carried out on rat and human samples. Rat liver, used as tissue positive control, showed a strong positive reaction at level of both rough endoplasmic reticulum and nucleus, mainly at the heterochromatin level (Fig. 1A). Rare

immunogold particles could be detected in the mitochondria. Negative controls, obtained omitting primary antibodies, showed no immunoreaction (Fig. 1B-D).

HRG immunogold analysis

TEM analysis of the three human skeletal muscle biopsies confirmed that muscle fibers were highly contracted as demonstrated by the narrow I bands (Fig. 2A).

The results of the immunogold analysis were comparable in the three biopsies. In particular, they evidenced the presence of HRG in the nuclei, in the sarcoplasmic reticulum and in the myofibrils (Fig. 2B-D). Only rare, occasional immunogold particles could be detected in the mitochondria while no immunoreaction could be localizable in the rough endoplasmic reticulum and in the Golgi apparatus. However, the majority of the protein was found within the myofibrils and in the nuclei. In particular, at sarcomeric level, HRG was mainly concentrated in the I-band although gold particles were also detectable in the actin containing portions of the A band (Fig. 2D). The semi-quantitative analysis confirmed this result as the density of the gold particles was significantly higher in the I-band than in the A-band (16.03 ± 4.16 and 6.7 ± 0.7, respectively; $P=0.0198$) (Fig. 2E).

A clear positive staining for HRG could also be evidenced in the nuclei where it localized almost exclusively in the heterochromatin (Fig. 2B). The HRG nuclear localization in the heterochromatin could suggest a nonspecific immunoreaction. In fact, as reported in literature (27), the fixation with glutaraldehyde and OsO_4 could ruin the antigens, therefore a nuclear background by immunogold particles could be observed over heterochromatin in osmicated muscle tissue. To rule out this event, further immunogold experiments were carried out using either 1% glutaraldehyde and post-fixing in 1% OsO_4 solution or 4% paraformaldehyde omitting the post-fixation step in 1% OsO_4 solution. Due to the difficulty in the availability of human samples, rat skeletal muscle was used for this purpose. Interestingly, we found the signal in the osmicated sections similar to the non-osmicated sections (Fig. 3A and B). In particular, in all the rat tested specimens the immunogold analysis evidenced the presence of HRG gold particles at nuclear level, confirming the pattern obtained in human samples, where the signal was localized mainly in the heterocromatin. Furthermore, in rat muscle fibers the immunogold particles were dispersed both in the intermyofibrillar spaces (sarcoplasmic reticulum) and

within the myofibrils. In particular, HRG was concentrated mostly at sarcomeric level and above all in the I-band (Fig. 3C and D), corroborating the observations made on the human samples.

HRG and AMPD1 double immunogold analysis

The co-localization of HRG and AMPD1 was analyzed on human skeletal muscle. A co-labeling of HRG and AMPD1 was evidenced in the sarcoplasmic reticulum, in the myofibrils (Fig. 4A) and in the nuclei (Fig. 4B). The percentage of HRG/AMPD1 co-localization was calculated respect to the total number of HRG gold particles. Three grids per each skeletal muscle biopsy were analyzed and 20 sarcomers/grid were observed. The average of co-localization in the sarcoplasmic reticulum and in the sarcomere was of 43% ± 24 and 44% ± 25, respectively. At nuclear level, the co-labeling of HRG and AMPD1 was found almost exclusively in the heterochromatin (7% ± 1).

To exclude an AMPD1 non-specific signal, possibly due to the use of the two primary antibodies both obtained in rabbit, additional immunogold experiments were performed using only the AMPD1 antibody. These experiments confirmed the pattern of positivity obtained with the double immunogold analysis (Fig 4C and D).

DISCUSSION

HRG is known to be a plasma protein that is synthesized by liver (1). We have previously demonstrated its presence in skeletal muscle, bound to the AMPD1 enzyme, giving the first evidence of a tissue localization of the protein (14). Moreover, we have shown that muscle cells do not synthesize HRG but they can internalize it from plasma (21). We have recently analyzed the localization of HRG in muscle fibers by confocal microscopy evidencing the protein in sarcoplasm, nuclei and mainly in myofibrils. (23). This microscopic technique allowed us to demonstrate that HRG is mainly concentrated in the I-band of the sarcomere; however, it was not sufficient to understand a more specific ultrastructural localization of the protein. The main purpose of the present immunohistochemical study was to deepen the ultrastructural localization of HRG in skeletal muscle fibers. The results obtained on human samples by TEM immunogold analysis evidenced the presence of HRG mainly in the heterochromatin of nuclei, in the sarcoplasmic reticulum and in the sarcomere.

In particular, at sarcomeric level HRG was mainly concentrated in the I-band although the gold particles were also detectable in the A-band. These results confirm those previously obtained with confocal laser microscopy by Mattii et al. (23) regarding the HRG localization in the I-band, but also reveal that HRG has a wider distribution in the sarcomere. In fact, at ultrastructural level, HRG was detectable not only in the I-band but also in the actin containing portions of the A band. Concerning the possible role of HRG in the sarcomere, we have already demonstrated its involvement, as Zn-metallochaperone, in the regulation of AMPD1. HRG could enhance the stability of AMPD1 in vivo through insertion of zinc or by modulating the intracellular zinc availability (16, 17). As a matter of fact, an immunohistochemical study performed on human skeletal muscle biopsies from patients with Primary and Acquired AMP deficiency has evidenced a positive correlation between the determined residual AMPD activity and the HRG abundance in the muscle specimens. The lower HRG polypeptide abundance observed in Primary AMP deficiency, that cannot be due to any pathological change except for the AMPD1 deficient background, suggests that there is a mutual dependence between skeletal muscle HRG and AMPD1 with regard to their stability (20). A similar role for HRG could also be speculated for other sarcomeric proteins that have zinc-binding sites such as Troponin T (28).

Concerning the HRG presence at level of SR vesicles, the data from literature highlighting the zinc involvement in intracellular signaling (29), support a role for the HRG protein in providing and regulate free Zn^{2+}, by virtue of its function as Zn-metallochaperone. Previous evidence suggests that the endoplasmic/sarcoplasmic reticulum seem to have a role also in Zn^{2+} storage (30), and a tight interplay may exist between Ca^{2+} and Zn^{2+} release events from this organelle. Moreover, in cardiac muscle Zn^{2+} may be able to bind to ryanodine receptor (RyR2) and modulate its function (31).

Zinc is a trace element essential for life (32). In normal cellular physiology, more than 99% of intracellular zinc is bound to proteins. The levels of free Zn^{2+} are very low and stringently regulated through the coordinated actions of zinc transporters, permeable channels and metallothioneins (MT) (33) since too little concentrations of zinc inhibit metabolism, whereas high concentrations are toxic to cells. MT serve as a storage site for Zn^{2+} and have chemical properties that support a dynamic role in

zinc trafficking. Nevertheless, zinc trafficking occurs in MT-null animals and cells indicating that other general routes of trafficking exist (34). HRG could be involved in one of these routes.

The HRG immunopositivity detected in the nuclei of human skeletal muscle was found almost exclusively in the heterochromatin. This new discovery, confirmed by control experiments on rat muscle fibers, is very intriguing as suggests a possible involvement of HRG in gene regulation. In fact, despite numerous data of literature report the involvement of HRG in a number of important biological processes such as cell proliferation, phagocytosis of apoptotic cells, angiogenesis, tumor progression, and show that all these activities are trigged in an indirect way, through HRG binding to cell surface molecules (e.g. glycosaminoglycans, tropomyosin, Fc receptors) (7,11,12,35), other study have already described HRG cell internalization (21, 22, 36) and demonstrated a cytoplasmic HRG localization (19, 23) and function (14, 16) in skeletal muscle. Even though the analysis of HRG amminoacidic sequence showed that HRG lacks the classical nuclear localization sequences that "tags" proteins for nuclear import, alternative nuclear localization mechanisms, that are likely to account for a large amount of nuclear traffic, could be involved in HRG nuclear localization (37). Studies are in progress to investigate the role of HRG in the nucleus.

None HRG localization was detected at level of rough endoplasmic reticulum and Golgi apparatus. We were not surprised to find it considering that HRG is not produced by skeletal muscle fiber but it is taken up from the circulation.

In the present paper, we have also investigated the co-localization of HRG and AMPD1 in human skeletal muscle fibers, since a relationship between the two proteins at this level has been previously demonstrated as above mentioned (14). Our ultrastructural analysis showed a co-labeling of HRG and AMPD1 in the sarcoplasmic reticulum, in the sarcomere and in the nucleus. The evidence of a co-localization of HRG and AMPD1 is not surprising thinking to the relationship between the two proteins (16, 23).

Interestingly, the present experimental work demonstrates for the first time the nuclear immunohistochemical localization of AMPD1 in human skeletal muscle. This finding corroborates a previous research that describes an AMPD activity in the nuclear fraction of rat brain (38).

Acknowledgments : We thank Mr Sauro Dini and Dr. Enza Polizzi for skillful technical support. Moreover, we thank Mrs. Petra Hrouzkova for English language proofreading.

Funding : This research was supported by a grant (PRA_2017_55) from the University of Pisa, Italy.

Competing Interests: The authors declare they have no competing interests.

Author Contributions:

All authors have contributed to this article as follows: LM designed and conducted experiments, analyzed data, created the figures and edited the manuscript; FB conducted experiments and analyzed data; AF conducted experiments and analyzed data; SF conducted experiments; MM conducted experiments; GA conducted experiments; GC conducted experiments ; ARMS conceived, designed, and coordinated research studies, conducted experiments, analyzed data and drafted the manuscript. All authors have read and approved the final manuscript.

Human and Animal Study Compliance:

All the procedures performed in the present study involving human participants were in accordance with the 1964 Helsinky Declaration and its later amendments. For this type of study, conducted retrospectively, formal consent was not required. The work on animals followed institutional, local, and national guidelines for animal experimentation. The investigation conforms with the Guide for the Care and Use of Laboratory Animals published by the US National Institutes of Health (NIH publication no. 85-23, revised 1996).

REFERENCES

1 Koide T, Foster D, Yoshitake S, Davie EW. Amino acid sequence of human histidine-rich glycoprotein derived from the nucleotide sequence of its cDNA. Biochemistry. (1986) 22; 25, 2220-5.

2 Hutchens TW, Yip TT, Morgan WT. Identification of histidine-rich glycoprotein in human colostrum and milk. Pediatr Res.(1992); 31, 239-46.

3 Leung LL, Harpel PC, Nachman RL, Rabellino EM. Histidine-rich glycoprotein is present in human platelets and is released following thrombin stimulation. Blood. (1983); 62:1016-21.

4 Sia DY, Rylatt DB, Parish CR. Anti-self receptors V. Properties of a mouse serum factor that blocks autorosetting receptors on lymphocytes. Immunology. (1982); 45:207-16.

5 Borza DB, Tatum FM, Morgan WT. Domain structure and conformation of histidine-proline-rich glycoprotein. Biochemistry. (1996);35:1925-34.

6 Morgan WT. Interactions of the histidine-rich glycoprotein of serum with metals. Biochemistry. (1981);20:1054-61.

7 Jones AL, Hulett MD, Parish CR. Histidine-rich glycoprotein binds to cell-surface heparan sulfate via its N-terminal domain following Zn^{2+} chelation. J Biol Chem. (2004);279:30114-22.

8 Jones AL, Hulett MD, Altin JG, Hogg P, Parish CR. Plasminogen is tethered with high affinity to the cell surface by the plasma protein histidine-rich glycoprotein. J Biol Chem. (2004);279:38267-76.

9 Gorgani NN, Parish CR, Altin JG. Differential binding of histidine-rich glycoprotein (HRG) to human IgG subclasses and IgG molecules containing kappa and lambda light chains. J Biol Chem. (1999);274:29633-40.

10 HeimburgerN, Haupt H, Kranz T, Baudner S. Human serum proteins with high affinity to carboxymethylcellulose. II. Physico-chemical and immunological characterization of a histidine-rich 3,8S-2-glycoprotein (CM-proteinI). Hoppe Seylers Z Physiol Chem. (1072);353:1133-40 (in German).

11 Gorgani NN, Altin JG, Parish CR. Histidine-rich glycoprotein regulates the binding of monomeric IgG and immune complexes to monocytes. Int Immunol. (1999);11:1275-82.

12 Guan X, Juarez JC, Qi X, Shipulina NV, Shaw DE, Morgan WT, McCrae KR, Mazar AP, Doñate F. Histidine-proline-rich glycoprotein (HRG) binds and transduces anti-angiogenic

signals through cell surface tropomyosin on endothelial cells. Thromb Haemost. (2004);92:403-12.

13 Jones AL, Hulett MD, Parish CR. Histidine-rich glycoprotein: a novel adaptor protein in plasma that modulates the immune, vascular and coagulation systems. Immunol Cell Biol. (2005);83:106-18.

14 Ranieri-Raggi M, Montali U, Ronca F, Sabbatini A, Brown PE, Moir AJG, Raggi A. Association of purified skeletal-muscle AMP deaminase with a histidine-proline-rich glycoprotein-like molecule. Biochem J. (1997);326:641-8.

15 Lowenstein JM, Tornheim K. Ammonia production in muscle:the purine nucleotide cycle. Science. (1971);171:397-00.

16 Ranieri-Raggi M, Martini D, Sabbatini AR, Moir AJ, Raggi A. Isolation by zinc-affinity chromatography of the histidine-proline-rich-glycoprotein molecule associated with rabbit skeletal muscle AMP deaminase. Evidence that the formation of a protein-protein complex between the catalytic subunit and the novel component is critical for the stability of the enzyme. Biochim Biophys Acta. (2003);1645:81-8.

17 Mangani S, Meyer-Klaucke W, Moir AGJ, Ranieri-Raggi M, Martini D, Raggi A. Characterization of the Zn binding site of the HPRG protein associated with rabbit skeletal muscle AMP deaminase. J Biol Chem. (2003);278:3176-84.

18 O'Halloran TV, Culotta VC. Metallochaperones, an intracellular shuttle service for metal ions. J Biol Chem. (2000);275:25057-60.

19 Sabbatini ARM, Ranieri-Raggi M, Pollina L, Viacava P, Ashby JR, Moir AJG, Raggi A. Presence in human skeletal muscle of an AMP deaminase-associated protein that reacts with an antibody to human plasma histidine-proline-rich glycoprotein. J Histochem Cytochem. (1999);47:255-60.

20 Sabbatini ARM, Toscano A, Aguennouz M, Martini D, Polizzi E, Ranieri-Raggi M, Moir AJG, Migliorato A, Musumeci O, Vita G, Raggi A. Immunohistochemical analysis of human skeletal muscle AMP deaminase deficiency. Evidence of a correlation between the muscle

HRG content and the level of residual AMP deaminase activity. J Muscle Res Cell Motil. (2006);27:83-92.

21 Sabbatini ARM, Mattii L, Battolla B, Polizzi E, Martini D, Ranieri-Raggi M, Moir AJ, Raggi A. Evidence that muscle cells do not express the histidine-rich glycoprotein associated with AMP deaminase but can internalize the plasma protein. Eur J Histochem. (2011);55:33-8.

22 Tugues S, Roche F, Noguer O, Orlova A, Bhoi S, Padhan N, Akerud P, Honjo S, Selvaraju RK, Mazzone M, Tolmachev V, Claesson-Welsh L. Histidine-rich glycoprotein uptake and turnover is mediated by mononuclear phagocytes. PLoS One (2014); 9:e107483 Erratum in: PloS One (2015);10:e0118636.

23 Mattii L, Rossi L, Ippolito C, Alì G, Martini D, Raggi A, Sabbatini ARM. Immunohistochemical localization of histidine-rich glycoprotein in human skeletal muscle: preferential distribution of the protein at the sarcomeric I-band. Histochem Cell Biol. (2017);148:651-7.

24 Dubowitz V, Brooke MH. Muscle Biopsy: A modern Approach. (1973) WB Saunders, London, Philadelphia, Toronto.

25 D'Alessandro D, Mattii L, Moscato S, Bernardini N, Segnani C, Dolfi A, Bianchi F. Immunohistochemical demonstration of the small GTPase RhoA on epoxy-resin embedded sections. Micron. (2004);35:287-96.

26 Moscato S, Cabiati M, Bianchi F, Vaglini F, Morales MA, Burchielli S, Botta L, Sabbatini ARM, Falleni A, Del Ry S, Mattii L. Connexin 26 Expression in Mammalian Cardiomyocytes. Sci Rep. (2018);8:13975-85.

27 Zuber C, Fan J, Guhl B, Roth J. Applications of immunogold labeling in ultrastructural pathology. Ultrastructural Pathology (2005); 29: 319-30.

28 Jin JP, Root DD. Modulation of troponin T molecular conformation and flexibility by metal ion binding to the NH2-terminal variable region. Biochemistry. (2000); 39:11702-11713.

29 Pitt SJ, Stewart AJ. Examining a new role for zinc in regulating calcium release in cardiac muscle. Biochem Soc Trans. (2015);43,:359–63.

30 Qin Y, Dittmer PJ, Park JG, Jansen KB, Palmer AE. Measuring steady-state and dynamic endoplasmic reticulum and Golgi Zn^{2+} with genetically encoded sensors. Proc. Natl. Acad. Sci. U.S.A. (2011);108:7351–56.

31 Diaz-Sylvester PL, Porta M, Copello JA. Modulation of cardiac ryanodine receptor channels by Alkaline earth cations. PLoS One (2011); 6: e26693.

32 Maret W. Zinc biochemistry: from a single zinc enzyme to a key element of life. Adv. Nutr. (2013);4: 82–91.

33 Colvin RA, Holmes WR, Fontaine CP, Maret, W. Cytosolic zinc buffering and muffling: their role in intracellular zinc homeostasis. Metallomics (2010); 2: 306–17.

34 Petering DH, Mahim A. Proteomic high affinity Zn^{2+} trafficking: where does metallothionein fit in? Int J Mol Sci.(2017);18:1289.

35 Chang NS, Leu RW, Rummage JA, Anderson JK, Mole JE. Regulation of macrophage Fc receptor expression and phagocytosis by histidine-rich glycoprotein. Immunology. (1992); 77:532-8.

36 Olsen HM, Parish CR, Altin JG. Histidine rich glycoprotein binding to T-cell lines and its effect on T-cell substratum adhesion is strongly potentiated by zinc. Immunology. (1996);88:198-06.

37 Lange A, Mills RE, Lange CJ, Stewart M, Devine SE, Corbett AH. Classical nuclear localization signals: definition, function and interaction with importin α. J Biol Chem. (2007); 282: 5101-5.

38 Manukian LA, Arutiunian AV. AMP-aminohydrolase activity of the nuclear fraction of rat brain. Vopr Biokhim Mozga. (1975); 10:33-9.

FIGURE LEGENDS

Figure 1

Controls for TEM immunogold analysis. (A) Tissue positive control: representative image of rat hepatocyte showing HRG immunopositivity at level of rough endoplasmic reticulum, mitochondrion and nucleus. (B-D) Negative controls: rat liver (B), rat skeletal muscle (C) and human skeletal muscle (D) did not show any immunoreaction. N: nucleus; RER: rough endoplasmic reticulum; SR: sarcoplasmic reticulum; M: mitochondrion. Scale bars: panels A and C=500 nm, panel B=200 nm, panel D=520 nm.

Figure 2

TEM immunogold analysis of human skeletal muscle. Pink A and yellow I capital letters indicate the A-band and I-band, respectively. (A) Representative image of a section counterstained with uranyl acetate and lead citrate. The sarcomeres are highly contracted (see the narrow I-bands). (B) Representative image of a nucleus of a muscle fiber showing a clear immunopositivity for HRG (arrows). Gold particles localize almost exclusively in the heterochromatin. C) Representative image of HRG immunopositivity (arrows) in sarcoplasmic reticulum (SR) and sarcomeres. D) Representative image of HRG immunopositivity in sarcomeres. Gold particles (20nm) are mainly localized at the I-band (arrows) and, in minor extent, in the A-band (arrowheads). (E) Density values of gold particles (mean number of gold particles/μm^2) in the sarcomeric I-band (δMV_I) and A-band (δMV_A). Error bars represent the standard deviation. The difference is statistically significant (*$P<0.05$). Scale bars: panels A, C and D=500 nm, panel B = 600 nm.

Figure 3

TEM immunogold analysis of rat skeletal muscle. Comparison of sections processed with and without the post-fixation step in 1% OsO_4 solution and incubated with anti-rat HRG antibody: the signal in the osmicated samples was similar to that observed in the non-osmicated sections. (A and B) Representative images of the nuclear positivity (arrows) obtained in osmicated (A) and in non

osmicated sections (B): in both samples the immunogold particles (10 nm, arrows) were localized almost exclusively in the heterochromatin. (C and D) Representative images of the sarcomeric positivity (arrows) obtained in osmicated (C) and in non osmicated sections (D): in both samples HRG was concentrated above all in the I-band. Gold particles were also detectable in sarcoplasmic reticulum (SR). Scale bars: panels A-D = 200 nm.

Figure 4

TEM immunogold analysis of HRG and AMPD1 in human skeletal muscle. (A and B) HRG-AMPD1 double immunogold: as pointed out by the arrows, HRG (20 nm gold particles) and AMPD1 (10 nm gold particles) co-localize in the sarcomere (A), in the sarcoplasmic reticulum (SR) (square in A) and in the heterocromatin of the muscle fiber nuclei (B). Arrowheads point to AMPD1 immunopositivity. (C and D) Representative image of AMPD1 immunopositivity (arrowheads): gold particles (10 nm) are localized in the sarcomere, in the sarcoplasmic reticulum (SR) and in the heterocromatin of the muscle fiber nucleus (N). Scale bars: panel A= 600 nm, panels B and D= 150 nm, panels C = 300 nm.

Figure 1

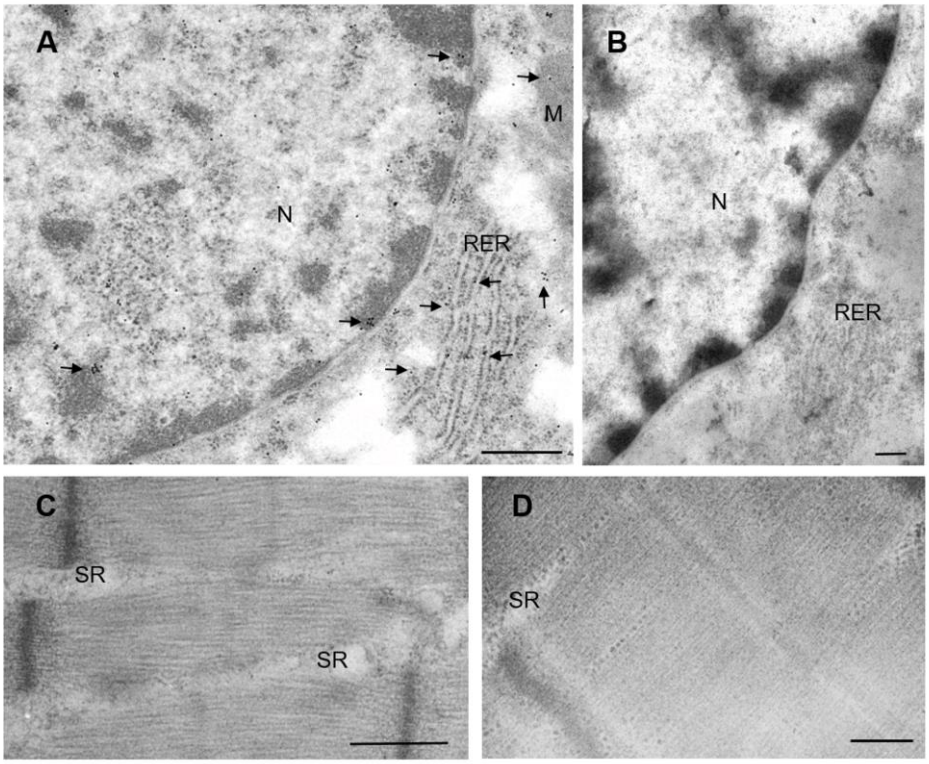

Figure 2

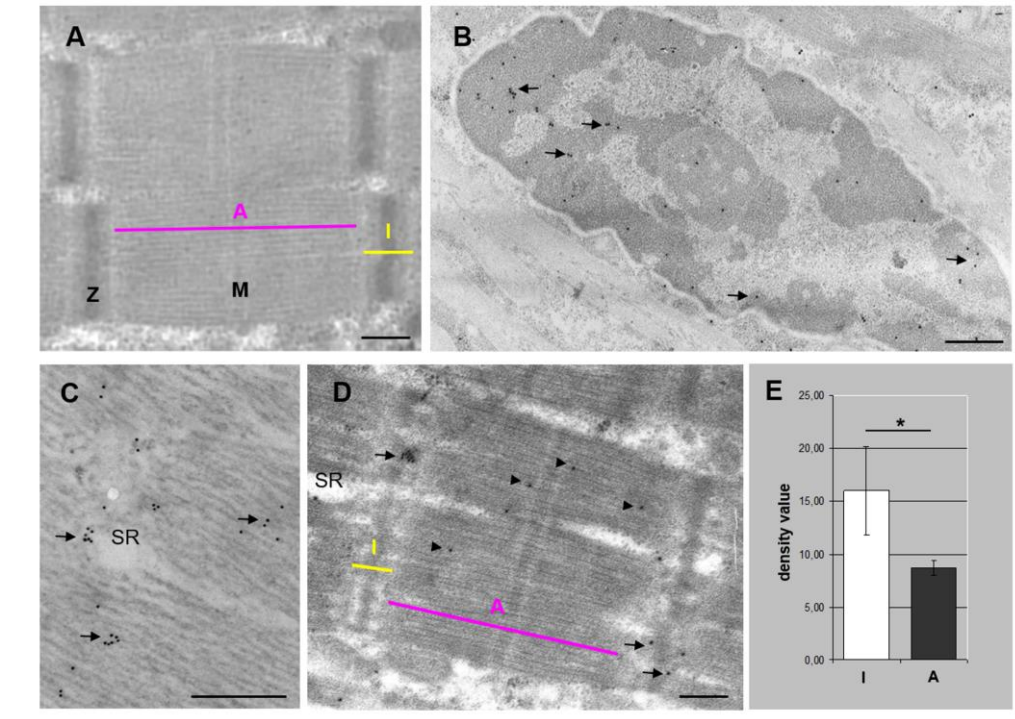

Figure 3

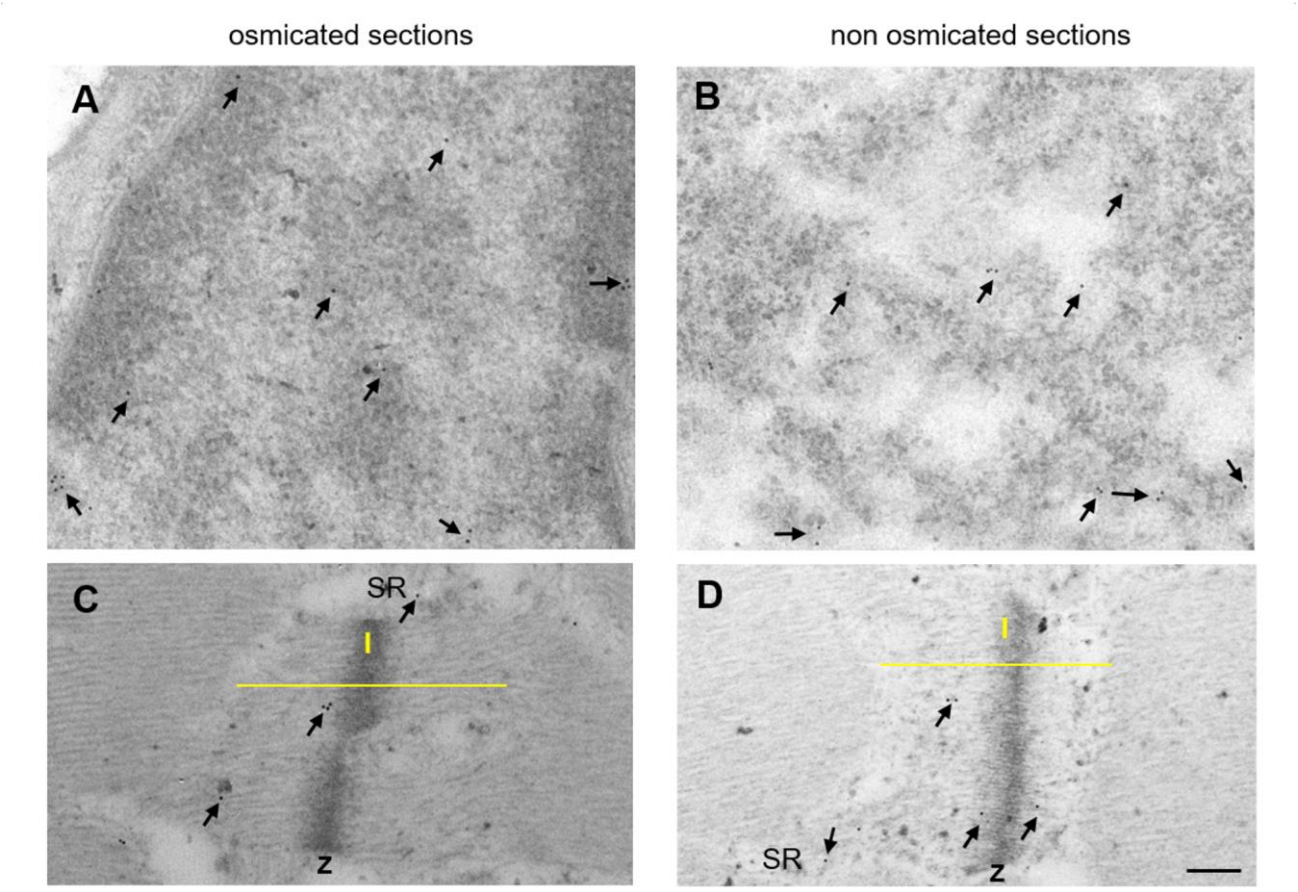

Figure 4